Simulation of Intramuscular EMG Signals Detected Using Implantable Myoelectric Sensors (IMES)

Madeleine M. Lowery*, *Member, IEEE*, Richard F. *ff.* Weir, *Member, IEEE*, and Todd A. Kuiken, *Member, IEEE*

***Abstract*—The purpose of this study was to test the feasibility of recording independent electromyographic (EMG) signals from the forearm using implantable myoelectric sensors (IMES), for myoelectric prosthetic control. Action potentials were simulated using two different volume conductor models: a finite-element (FE) model that was used to explore the influence of the electrical properties of the surrounding inhomogeneous tissues and an analytical infinite volume conductor model that was used to estimate the approximate detection volume of the implanted sensors. Action potential amplitude increased progressively as conducting electrodes, the ceramic electrode casing and high resistivity encapsulation tissue were added to the model. For the muscle fiber locations examined, the mean increase in EMG root mean square amplitude when the full range of material properties was included in the model was 18.2% ($\pm 8.1\%$). Changing the orientation of the electrode with respect to the fiber direction altered the shape of the electrode detection volume and reduced the electrode selectivity. The estimated detection radius of the IMES electrode, assuming a cylindrical muscle cross section, was 4.8, 6.2, and 7.5 mm for electrode orientations of 0°, 22.5°, and 45° with respect to the muscle fiber direction.**

***Index Terms*—Detection volume, EMG, encapsulation tissue, implantable electrode, myoelectric prostheses.**

I. Introduction

CONVENTIONAL myoelectric prostheses utilize surface electromyographic (EMG) signals recorded above large superficial muscles to control a prosthetic device. The advantages of myoelectric control include its noninvasive nature and the relative ease with which it can be applied. Where possible, EMG signals are used to control movements which relate directly to the original function of the muscle from which they are recorded, resulting in a relatively intuitive feel for the user. Current clinically available prostheses, however, are limited to one or two degrees of freedom (DOF) devices that can only be controlled in a sequential manner. A major effort in prosthetics research is, therefore, currently directed towards developing means to simultaneously control multiple DOF of upper limb prostheses. Light-weight, multifunctional hand prostheses have the potential to allow the fingers and thumb to move independently [1]–[4]. However, their practical application remains limited by the number of control signals that are available. Current commercially available artificial hands, therefore, have only a single degree of freedom which allows them to open and close, but does not enable them to achieve the multiple grip patterns needed in everyday tasks [3].

The manipulation capabilities of the human hand are governed by the activation patterns of the many muscles of the forearm and hand. Many of these muscles lie deep within the forearm and are relatively small in size. For this reason, there are only a small number of superficial forearm muscles from which surface EMG signals can reliably be detected. Furthermore, the relatively small size and close proximity of the forearm muscles to one another means that cross-talk from adjacent or deep muscles is often a concern. This problem is further exacerbated if there are significant amounts of subcutaneous fat tissue between the muscle and the recording electrodes [5].

An implanted electrode system is currently being developed to record multiple intramuscular EMG signals from small muscles in the forearm to control multifunction hand prostheses [6]. The control system will be capable of detecting, receiving and processing EMG signals from up to 16 implanted myoelectric sensors (IMES), potentially controlling a device with eight or more DOF. Each IMES will be packaged in a RF BION® hermetically sealed ceramic capsule provided by the Alfred E. Mann Foundation (Valencia, CA). The capsules are small enough to be injected through a 12-gauge hypodermic needle and are capped on either end with two titanium alloy electrodes which form the recording surfaces of the bipolar EMG sensor. The intramuscular EMG signals detected with the IMES recording and telemetry system will enable signals to be recorded from small and deep muscles such as the extrinsic hand muscles of the forearm, thereby greatly increasing the number of signals available to control a prosthetic device.

While the characteristics of conventional surface EMG signals have been widely studied using experimental and simulation methods, the characteristics of intramuscular EMG signals have received considerably less attention. In addition, due to the constraints imposed by the capsule in which the electronics and transmitter are contained, the interelectrode distance and geometry of the implanted recording electrode are substantially different than those of conventional intramuscular fine-wire or needle electrodes used to record motor unit and muscle fiber activity. Typical recording surfaces for fine-wire or needle EMG electrodes are 25–300 μm in diameter, with an interelectrode distance of a similar order of magnitude [7]. Due to the small electrode size and interelectrode spacing, the amplitude of the

Manuscript received April 1, 2005; revised September 11, 2005. This work was supported by the National Institute of Child and Human Development under Grant RO1 HD043137-03. *Asterisk indicates corresponding author.*

*M. M. Lowery is with the School of Electrical, Electronic and Mechanical Engineering, University College Dublin, Belfield, Dublin 4, Ireland (e-mail: madeleine.lowery@ucd.ie).

R. F. *ff.* Weir is with the Neural Engineering Center for Artificial Limbs, Rehabilitation Institute of Chicago, Chicago, IL 60611 USA. He is also with the Department of Physical Medicine and Rehabilitation, Northwestern University, Chicago, IL 60611-4496 USA and the Jesse Brown VA Medical Center —Lakeside CBOC, Chicago, IL 60611-4496 USA (e-mail: rweir@northwestern.edu).

T. A. Kuiken is with the Neural Engineering Center for Artificial Limbs, Rehabilitation Institute of Chicago, Chicago, IL 60611 USA and also with the Department of Physical Medicine and Rehabilitation, Northwestern University, Chicago, IL 60611-4496 USA (e-mail: tkuiken@northwestern.edu).

Digital Object Identifier 10.1109/TBME.2006.881774

detected intramuscular action potentials decreases rapidly with increasing distance of the muscle fibers from the recording electrode. The intramuscular fine-wire or needle electrode is, therefore, highly selective, enabling action potentials from individual motor units to be discriminated. Previous simulation studies have estimated that 80% of the area of the motor unit action potential detected with concentric needle electrodes is produced by muscle fibers lying within 1.5–2 mm of the electrode [8].

In contrast, the recording surface of the IMES electrode is 2.5 mm diameter, with an interelectrode spacing of 14.5 mm, considerably larger than the recording surface and interelectrode distance of intramuscular electrodes. Given the larger recording surface and interelectrode distance, it is likely that the detection volume of the IMES is substantially larger than that of conventional intramuscular EMG electrodes. However, it is not clear how large this detection volume is, or whether cross-talk between adjacent muscles is likely to impede the detection of independent EMG signals from neighboring muscles.

The inflammatory response of the body to implanted electrodes leads to the formation of fibrocollagenous tissue around the electrode. The properties of this capsule depend on the biocompatibility of the implant which is determined by features such as the implant shape, surface texture and material composition [9]. Tests on implanted BION® stimulation devices, with similar casing to the IMES examined here, have indicated the formation of compact laminated layers of 50–100 μm thick fibrocollagenous tissue surrounding devices implanted in rat hind-limb muscles [10]. The presence of encapsulation tissue has been shown to alter the spatial distribution of the electrical field around implanted stimulation electrodes and in some cases to impede the stimulation of target nerve fibers [9] and alter the resulting electrode recruitment profile [11]. Surface EMG simulation studies have indicated that the presence of highly resistive tissues, such as subcutaneous fat or bone, in the vicinity of the recording electrode results in a distortion of the surrounding electric field and can affect detected surface EMG signals [12]. It is likely that the presence of the electrode casing and the formation of high resistivity encapsulation tissue modify the flow of current in the vicinity of the electrode. It is also possible that these highly resistive materials may impede the detection of EMG signals at the implanted electrode.

The purpose of this study was to develop a realistic model of an implanted IMES electrode with which to examine the effect of inhomogenous materials, in particular the nonconducting electrode casing and high resistivity encapsulation tissue and estimate the approximate detection volume of the implanted electrode. The effect of varying the orientation with respect to the muscle fiber direction was also examined. The detection volume of the electrode is important in determining whether the IMES may be used to detect independent EMG signals from adjacent muscles to control separate functions of a myoelectric prosthesis.

II. Methods

Two models were used to examine volume conduction of EMG signals detected by the intramuscular IMES electrode. The first model was a detailed finite-element (FE) model that incorporated the electrode dimensions and the electrical properties of the surrounding inhomogeneous tissues and electrode casing. In the second, analytical model, muscle fibers were located in homogenous anisotropic muscle tissue of infinite extent and the electrodes were approximated as point electrodes. The rate at which the EMG signal decayed with increasing distance of the muscle fibers from the electrode in both models was compared. The homogeneous, infinite volume conductor model was then used to examine the detection volume of the implanted electrode during simulated simultaneous activation of large numbers of motor units.

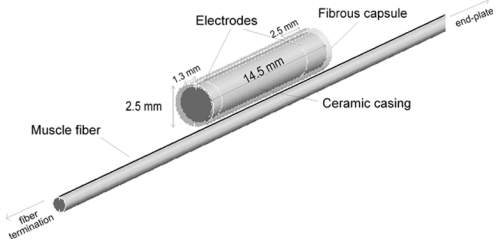

Fig. 1. Geometry of FE model in the region of the electrode, illustrating the electrode geometry, fibrous capsule, and a representative muscle fiber.

A. Finite-Element Model

The FE model meshes were generated and the potential throughout the model solved using the Ansoft EMAS software package (EMAS 4.1, Ansoft Corp., Pittsburgh, PA). The dimensions of the simulated implanted electrode were based on measurements of the IMES electrode. The recording electrode consisted of a ceramic cylinder casing, 2.5 mm diameter, in which the electronic components for recording and transmission would be contained. The casing was capped at each end with a conducting metal electrode. The total length of the cylinder, including the electrodes, was 14.5 mm. Consistent with the physical dimensions of the IMES, the electrode poles were asymmetrical, 2.5 and 1.3 mm long, respectively, Fig. 1.

In vivo tests on implanted BION® stimulation devices housed in the same casing as the IMES electrodes examined here, indicate the formation of compact laminated layers of fibrocollagenous tissue, 50–100 μm thick, surrounding devices implanted in rat hind limb muscles [10]. The formation of the fibrocollagenous tissue is most likely due to the interaction of the implants with the surrounding tissue, rather than an electrochemical by-product of the stimulation, as similar stimulation thresholds and encapsulation tissue formation were observed with both implanted active and inactive BION® devices [10]. Grill and Mortimer [9] earlier reported the thickness of encapsulation tissue surrounding chronically implanted silicon and epoxy electrode arrays to be 808 μm and 446 μm, respectively. For this simulation study the thickness of the encapsulation tissue was chosen to be 250 μm, between the experimental values reported in these two studies, and representing a likely upper-bound on the encapsulation tissue thicknesses that may occur due to implantation of the IMES. The electrode and fibrous capsule were embedded in a sphere of cylindrically anisotropic muscle tissue 200 mm radius. The FE mesh was generated using three-dimensional (3-D), linear, tetrahedral elements. The distance between adjacent nodes of the mesh

varied from 0.1 mm, along the muscle fiber, to 10 mm elsewhere in the volume conductor. Care was taken to confirm that further reducing the size of the mesh elements did not alter the voltage at the recording electrodes.

The electric field, $\overrightarrow{E}$, in the volume conductor is described by Maxwell's equation derived from Ampere's Law in point form

$$\nabla \cdot \left(\varepsilon \frac{\partial \overrightarrow{E}}{\partial t} + \sigma \overrightarrow{E} \right) = 0 \tag{1}$$

where σ is the conductivity and ε is the permittivity of the medium. $\overrightarrow{E}$ is a gradient field, i.e., $\overrightarrow{E} = -\nabla\phi$, where ϕ is the electric scalar potential. The electrical potential throughout the model was solved assuming that the muscle tissue extended infinitely. This assumption is reasonable if the muscle fibers are assumed to lie sufficiently far from the interface of the muscle and fat tissue. This was implemented by applying boundary conditions based on Bayliss-Turkel approximations on the surface of the FE model [13].

1) Source Description: The muscle fiber action potential source was modeled as line of point current sources, obtained by discretizing the second derivative of the transmembrane action potential described analytically by Rosenfalck [14], at 0.1 mm intervals between 0 and 38 mm, scaling appropriately [14] and removing the mean so that the sum of the point current sources was equal to zero. The point current sources were applied at a series of nodes separated by a distance of 0.1 mm along the muscle fiber. The potential at the recording electrode was calculated for each muscle fiber location, at each time step, as an action potential propagated along the muscle fiber in both directions away from the muscle fiber end-plate with a conduction velocity of 4 m/s. Fiber length in the muscles of the human forearm range from approximately 142 and 108 mm in the in the brachioradialis and extensor carpi radialis muscles, respectively, to 45 and 38 mm in the extensor pollicis longus and flexor pollicis longus muscles [15]. A muscle fiber length of 100 mm was simulated, with the muscle fiber endplate located midway along the fiber. The electrode was positioned midway between the endplate and the fiber termination, orientated with the larger electrode pole located proximal to the endplate, Fig. 1.

Muscle fiber start and end effects were incorporated by applying compensating currents at the fiber end-plate during the action potentials initiation and at the fiber terminations during action potential extinction. The compensating currents were equal in magnitude and opposite in sign to the integral of the applied current along the fiber, thus ensuring that the total current in the model was equal to zero at all times [16], [17].

2) Material Properties: The frequency content of the intramuscular EMG signal falls within the alpha dispersion range for biological tissues, with muscle permittivity decreasing as frequency increases [18]. There is considerable variability among the relative permittivity values that have been reported for biological tissues [18] and currently available solvers do not incorporate low frequency dispersion. Muscle conductivity and permittivity were, therefore, considered to be constant at the frequencies of interest, although the absence of frequency dispersion with respect to the permittivity could cause the contribution of the tissue capacitive effects to be overestimated [19]. Conductivity and relative permittivity values for muscle were chosen from experimental data reported at 300 Hz in [20], as this was the approximate mean value of the median frequency of simulated intramuscular action potentials calculated during preliminary studies. The muscle tissue was assigned a conductivity of 0.3 S/m in the direction transverse to the muscle fiber and 0.4 S/m parallel to the fiber [20]. Relative permittivity was 6×10^6 and 1.5×10^7 in the transverse and longitudinal muscle directions, respectively. The electrode casing was assigned a conductivity of 1×10^{-15} $\mathrm{S/m}$ and a relative permittivity of 4.6. The conductivity of the electrodes was 1×10^7 $\mathrm{S/m}$ with relative permittivity of 1.

The encapsulation tissue surrounding a biocompatible implanted device is composed of a tightly packed layer of collagen, fibroblasts and small macrophages and lymphocytes. The layer surrounding a less biocompatible device consists of a larger, looser matrix of collagen and fibroblasts, with an increased level of mononuclear cell infiltration [9], [10]. There is relatively little data available on the electrical properties of collagen. Experimental measurements of the electrical properties of encapsulation tissue in cat muscle report frequency independent resistivity with a mean value of 627 Ω–cm around silicone rubber electrode arrays and a slightly lower, frequency dependent, resistivity of 454–193 Ω–cm for the encapsulation tissue around epoxy arrays [9], with negligible reactive component in the tissue surrounding both arrays. Sahakian *et al.* [21] used a conductivity of 0.025 S/m to model fibrotic tissue inhomogeneities in cardiac muscle tissue. The thin 50–100 $\mu\mathrm{m}$ encapsulation layer observed around the casing of BION® stimulation devices implanted in rat hind-limb muscles and the high bio-compatibility of ceramic materials suggests that the resistivity of the fibrocollagenous tissue surrounding the IMES devices may be even higher than that reported by Grill and Mortimer [9]. A conductivity of 0.025 S/m was, therefore, chosen for the encapsulation tissue in the model. This represents the lower end of the range of conductivity values likely to occur in the region around the implanted electrode. The encapsulation tissue was assigned a relative permittivity of 1.

3) FE Model Simulation Details: Action potentials were simulated using a time step of 0.25 ms. Simulations were conducted for muscle fibers located 1.75, 2, 3, 5, 7, and 10 mm from the center of the electrode. Effects due to the electrode casing, the surrounding encapsulation tissue and the electrode geometry were examined by replacing each material in turn with muscle tissue.

B. Analytical Infinite Volume Conductor Model

The analytical infinite volume conductor model calculates the potential at a point electrode due to an action potential propagating along a fiber located in a cylindrically anisotropic homogeneous muscle model of infinite extent [17], [22]. The electrical potential, ϕ, at a point in the conductor due to a point current source, I, is given by [22]–[24]

$$\phi = \frac{1}{4\pi\sigma_t} \frac{I}{\sqrt{\frac{\sigma_z}{\sigma_t} r^2 + z^2}} \tag{2}$$

where r is the radial distance between the fiber and the observation point, and z is the axial distance between the observation

point and the point current source. σ_t and σ_z are the conductivities of the muscle tissue in the directions transverse and parallel to the muscle fiber, respectively. In the analytical volume conductor model the 3-D electrodes were approximated by point electrodes located at the midpoint of the outer surface of the electrode poles. The potential at the electrode was calculated with a time step of 0.25 ms as action potentials propagated along the muscle fiber with a conduction velocity of 4 m/s.

The current source representation, generation and termination of the action potentials, muscle fiber diameter, muscle fiber conduction velocity and electrode locations were the same as for the FE model simulations.

1) Simulation of Voluntary EMG Activity: To simulate signals representative of EMG data recorded when large numbers of motor units are simultaneously active such as during voluntary contraction, motor unit action potentials were simulated for 1000 motor units using the analytical infinite volume conductor model. The centers of the motor unit territories were randomly distributed throughout a circular cross section of 15 mm radius. The IMES electrode was located at the center of the active muscle territory. Each motor unit was composed of 400 simultaneously activated muscle fibers distributed randomly within a 2.52 mm radius about the center of the motor unit territory, assuming a muscle fiber density of 20 $\mathrm{fibers/mm^2}$ [25]. This is consistent with a mean motor unit territory diameter of 5.5 mm reported for the extensor digitorum communis muscle [26]. Motor unit territories were allowed to overlap. Muscle fiber end-plates were randomly distributed throughout the motor unit end-plate zone which was 10 mm wide, located mid-way along the muscle fiber. The fiber terminations were similarly randomly distributed throughout 10 mm wide regions centered on both ends of the fiber. Each motor unit action potential was calculated at each time step as the total potential at the electrodes due to the propagation of action potentials along each of the muscle fibers in the motor unit. Further details of the analytical model are given in [27].

Variations in motor unit type, size, fiber diameter, muscle fiber conduction velocity, motor unit firing rate and synchronization between the firings of simultaneously active motor units all affect EMG signal amplitude. To exclude effects due to variations in motor unit type, motor unit type was assumed to be uniform across the muscle. All motor units were assigned the same mean firing rate and motor units were assumed to fire independently of one another. In the simulated data presented here, each motor unit discharged with a mean interpulse interval of 50 ms with standard deviation of 6.275 ms [28], corresponding to a mean firing rate of 20 Hz.

2) Analytical Model Simulation Details: To compare the rate of action potential decay in the analytical and FE models, action potentials were first simulated using the same muscle fiber locations as in the FE simulations. The relative contribution of muscle fibers located throughout the muscle cross sectionwas then investigated by simulating action potentials from 20 000 muscle fibers randomly located within a 15 mm radius of the center of the IMES electrode. Finally, to estimate the approximate detection volume of the IMES electrode, the electrode detection radius was defined as the radius of muscle for which the simulated EMG root mean square (RMS) amplitude was equal

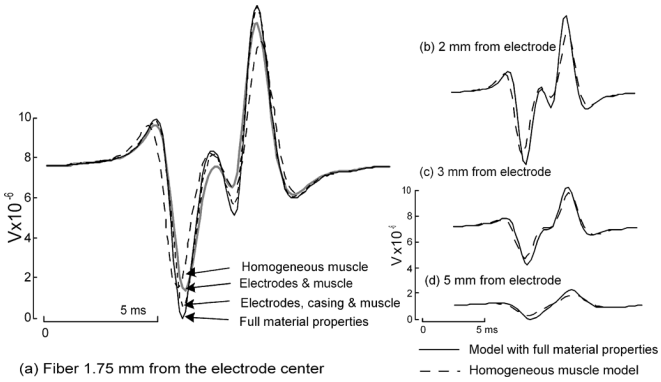

Fig. 2. Comparison of intramuscular bipolar action potentials simulated with four different models: (i) homogeneous muscle model (ii) model with muscle and electrodes (iii) model with muscle, electrode and casing (no fibrous tissue) (iv) model with full material properties (muscle, casing, fibrous encapsulation tissue and electrodes). Action potentials are presented for muscle fibers located 1.75, 2, 3, and 5 mm from the center of the electrode surface.

to 90% of the amplitude of the signal detected when all 1000 motor units were active. The detection radius was estimated by calculating the RMS amplitude of the simulated EMG signal as the radius of the active muscle was progressively increased, while keeping the motor unit distribution constant. The RMS value of the resulting EMG signal was compared with the RMS value of the EMG signal detected when all motor units were active. Assuming that the firing times of simultaneously active motor units are uncorrelated and that the motor unit action potential trains are of zero mean the variance of the resulting EMG signal is equal to the sum of the variance of the contributing motor unit action potential trains [27]. In this case, the 90% RMS detection radius corresponds to the region of muscle from which 81% of the EMG signal power originates.

III. Results

A. Effect of Encapsulation Tissue and Electrode Casing

Examples of muscle fiber action potentials simulated using the finite element model for different combinations of material properties are presented in Fig. 2. When compared with action potentials simulated using a model composed of homogenous muscle tissue, action potential amplitude increased progressively as conducting electrodes, the electrode casing and the highly resistive encapsulation tissue were added to the model, Fig. 2(a).

The increase in action potential amplitude was observed for all fiber locations and was greatest for muscle fibers located closest to the electrode. For a muscle fiber located 1.75 mm from the center of the electrode (0.25 mm from the edge of the fibrous capsule), the RMS amplitude of the action potential simulated using the full FE model with electrodes, casing and encapsulation tissue was 20.8% greater than that simulated using the homogeneous muscle model. The relative contribution of each inhomogeneous tissue to the amplitude increase may be seen by considering the increase observed as each material was added to the model. The addition of conducting, 3-D electrodes to the homogeneous muscle model resulted in a 6.7% increase in RMS amplitude for the fiber located 1.75 mm from the center of the

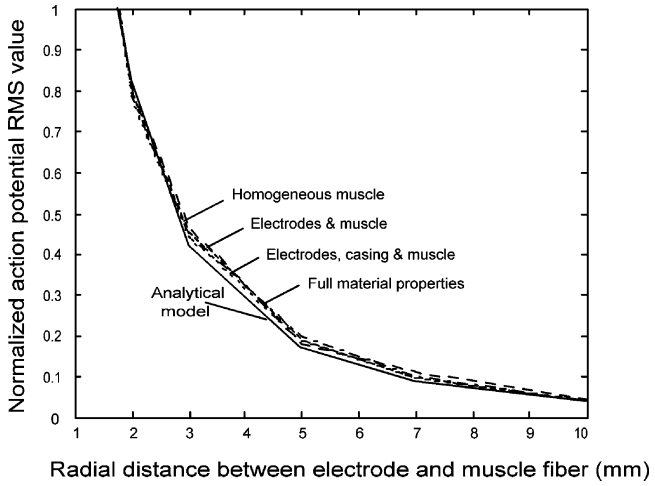

Fig. 3. Rate of decay of simulated action potential RMS amplitude with increasing distance from the IMES electrode. Results are compared for action potentials simulated using the analytical model, the FE model with full material properties, the FE model with electrodes and casing, the FE model with electrodes only and the homogenous muscle FE model.

electrode. The highly resistive casing caused a 10.25% increase in action potential RMS amplitude, while the RMS amplitude increase observed when the fibrous capsule was added to the model was relatively small, 3.9% in this example, Fig. 2. A progressive increase in action potential amplitude with the addition of conducting electrodes, the casing and fibrous encapsulation tissue was similarly observed for all muscle fiber locations examined.

B. Rate of Decay of Action Potential Amplitude

To examine the rate of decay of the action potential amplitude with increasing distance from the electrode, the RMS values of simulated action potentials were normalized with respect to the maximum action potential amplitude, Fig. 3. Despite the variation in EMG amplitude with the material properties of the surrounding tissues, Fig. 3, the rate of decay of the EMG amplitude was similar in all models. Furthermore, the rate of decay of the EMG amplitude was well approximated by the analytical EMG model, Fig. 3.

C. Detection Volume of Implanted Electrodes

As the rate of decay of the EMG amplitude was reasonably well approximated by the analytical volume conductor model, this model was used to further examine the selectivity and detection volume of the IMES electrode. Isopotential contours indicating the RMS amplitude of single muscle fiber action potentials detected from fibers located throughout the muscle tissue are illustrated in Fig. 4. The isopotential contours describe muscle fiber locations for which action potentials of equal RMS amplitude are detected at the electrode. The contour plots were generated based on simulations of 20 000 muscle fibers randomly located throughout the muscle tissue. Values are presented for electrodes orientated parallel to the muscle fiber, and orientated 22.5° and 45° with respect to the muscle fiber direction. The amplitude of each action potential has been normalized with respect to the maximum action potential amplitude detected with that electrode configuration.

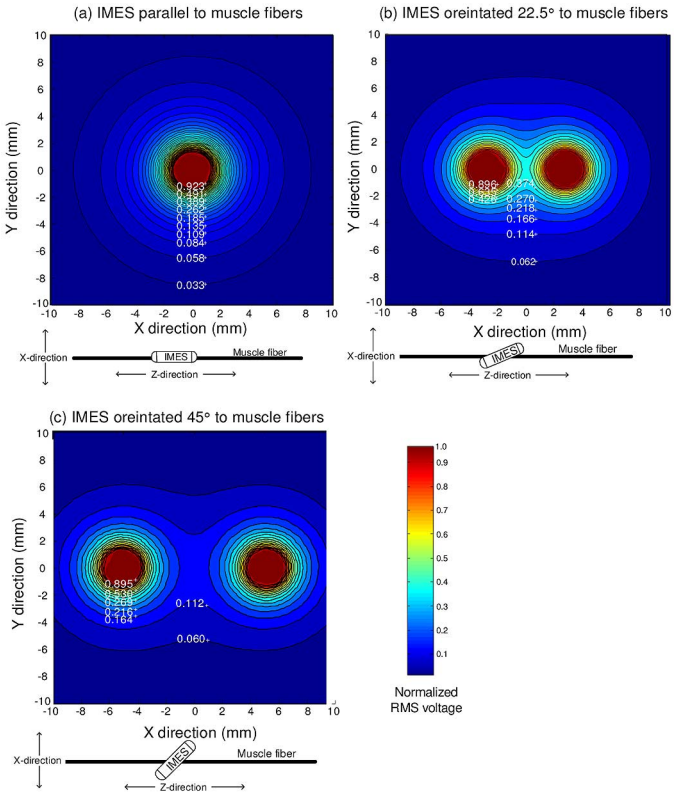

Fig. 4. RMS value of action potentials detected at the IMES electrode for muscle fibers at 20 000 different locations throughout the muscle cross section. The mid-point of the longitudinal axis of the IMES electrode was located at X, Y co-ordinates (0, 0). Values are presented for (a) the electrode orientated parallel to the muscle fiber direction, (b) the electrode orientated 22.5° with respect to the fiber direction, and (c) the electrode orientated 45° with respect to the fiber direction. The RMS values have been normalized with respect to the maximum RMS value detected for that electrode orientation. Each isopotential line represents muscle fiber locations for which the RMS value of the action potential detected at the electrode are constant. The muscle fiber direction is perpendicular to the page, the X-direction represents the muscle width and the Y-direction the muscle depth. The smaller diagram below each figure illustrates the corresponding orientation of the IMES along the Z and X axes. (Color version available online at http://ieeexplore.ieee.org).

Voluntary EMG signals were then simulated for large numbers of repetitively firing motor units distributed throughout the muscle cross section. An example of a simulated EMG signal is presented in Fig. 5(a) for a muscle of radius 5 mm and electrode orientation of 22.5°. EMG signals were simulated as the radius of the active muscle was progressively increased, while keeping the motor unit distribution constant. The RMS values of the simulated EMG signals are presented in Fig. 5 for increasing muscle radius. Data are presented for each electrode orientation. EMG amplitude was calculated for 1-s epochs and normalized with respect to its maximum value, when all motor units were active.

The effective detection radius of the IMES electrode was defined as the radius of muscle for which the EMG RMS amplitude was 90% of the RMS value when all motor units were active. The effective detection radius was 4.8, 6.2, and 7.5 mm when the IMES was orientated 0° (parallel), 22.5°, and 45° with respect to the muscle fiber direction, respectively, Fig. 5(b).

A direct comparison of the electrode detection radius with muscle cross sectional area across the different forearm mus-

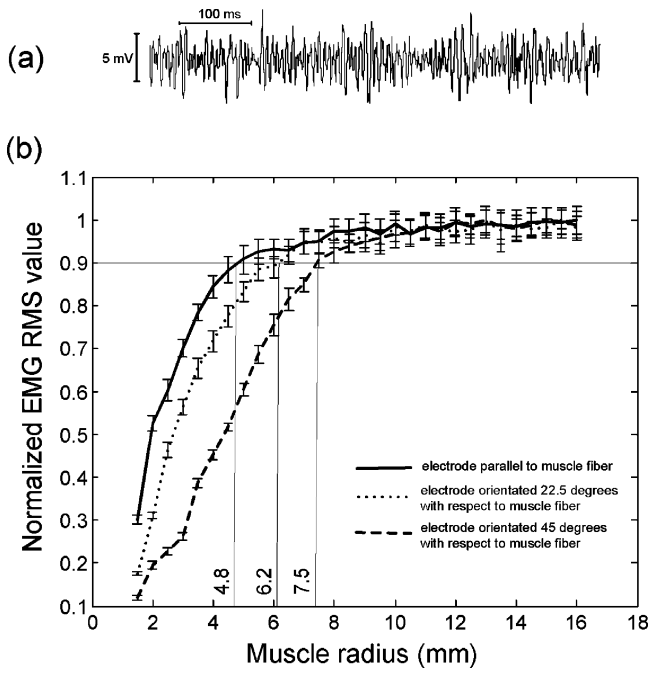

Fig. 5. (a) Sample EMG signal simulated for electrode orientation of 22.5° and muscle radius of 5 mm. (b) RMS value of simulated EMG signals for different values of the muscle radius, assuming a cylindrical muscle volume. Values are presented for different electrode orientations. The RMS values were normalized with respect to the maximum EMG RMS value with that electrode orientation. The effective detection radius of the electrode is estimated as the radius at which the RMS value of the EMG signal is 90% of that detected when all motor units were active. The mean and standard deviation of 10 simulations are presented.

cles is difficult due to variations in muscle architecture. Based on measurements of muscle physiological cross sectional area from the literature and assuming a circular muscle cross section, approximate values for the muscle radius in the extensor pollicis longus, flexor carpi radialis and flexor carpi ulnaris muscles are 5.2–5.6, 8–9.6, and 10.4–13.8 mm [15], [29]. To further compare the estimated electrode detection radius to the size of the forearm muscles the detection radius is presented along with an illustration of the cross sectionof the human forearm [30], scaled to the dimensions of the forearm of a typical male subject, Fig. 6.

IV. Discussion

There is currently a large amount of interest in implanted neuromuscular stimulation and sensing devices. However, there is no quantitative data on the theoretical detection range of chronically implanted EMG sensors. The purpose of this study was to examine the detection volume of implanted IMES and to explore the influence of the electrode casing, highly resistive encapsulation tissue and the electrode orientation. Two different modeling methods were used to examine these issues. The effects due to the conductivities and permittivities of the electrode, its casing and the encapsulation tissue were examined using FE models that allow complex geometries and tissue inhomogeneities to be simulated. The rate of EMG decay and the detection volume of the electrode were then examined using an analytical model, since the rate of decay of EMG amplitude with increasing distance from the electrode was found to be similar in both models, Fig. 3. The analytical infinite volume conductor model is computationally efficient, enabling large numbers of muscle fibers

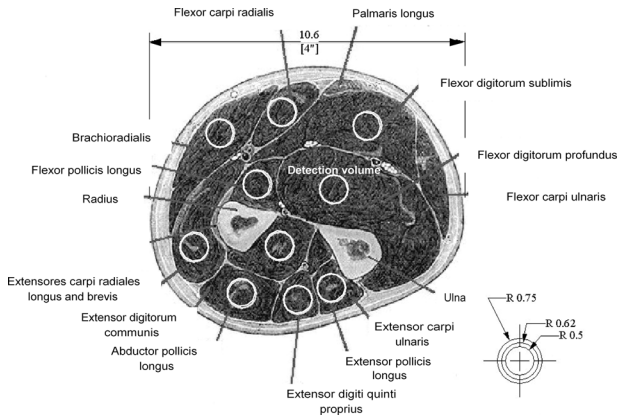

Fig. 6. Cross sectionthrough the middle of the forearm indicating the estimated detection radius of IMES electrodes orientated parallel to the muscle fiber direction. The image, adapted from [30], is scaled based on the forearm radius of a typical male subject.

and motor units to be simulated, but does not take account of variations in tissue properties or model geometry.

The presence of encapsulation tissue around the implanted electrode caused an increase in action potential amplitude, Fig. 2. When compared with action potentials simulated in a homogeneous muscle model, action potential amplitude increased progressively as conducting electrodes, a ceramic electrode casing and high resistivity encapsulation tissue were added to the model. The increase in action potential amplitude with the addition of a high resistively layer around the electrode may seem initially counterintuitive. However, it is consistent with previous surface EMG simulation studies which have shown an increase in surface EMG amplitude when a layer of muscle tissue beneath the electrode was replaced with more resistive fat tissue [12], [31]. The high resistivity tissue restricts current flow in the region surrounding the electrode, causing the voltage at the interface of the high resistivity encapsulation tissue to increase. Due to the small amount of current entering the region of high resistivity tissue, the voltage dropped across that region is relatively low, yielding a net increase in the potential observed at the recording electrode. Most of the observed increase in EMG amplitude was due to the presence of the nonconducting capsule on which the electrodes are mounted, Fig. 2. The capsule similarly restricts current flow in the vicinity of the electrodes, increasing the current density in this region.

In myoelectric control paradigms where activation of each muscle controls a different function of the prosthesis, it is desirable that cross-talk between neighboring muscles is minimized, as high levels of cross-talk may result in incorrect activation of the device. Surface EMG cross-talk is known to vary with electrode configuration, subcutaneous fat thickness and muscle anisotropy [5], [12], [32]. Orientation of the electrode with respect to the fiber direction also alters EMG selectivity, with the most selective EMG recordings obtained by aligning the electrodes along the fiber direction. In the simulated data, the selectivity of the bipolar electrode was substantially reduced when the electrode was not orientated parallel to the muscle fiber, Fig. 5(b). The shape of the isopotential contours describing fiber locations which contribute equally to the EMG amplitude also varied with electrode orientation, Fig. 4. The sensor was most

sensitive to muscle fibers located next to either electrode pole, yielding two high-sensitivity areas, Fig. 4. Increasing the offset of the electrode axis from the fiber direction further broadened the detection volume of the electrode.

While a comparison of action potential amplitudes from different fibers provides an indication of the rate of EMG decay with increasing distance of the fiber from the electrode, it is difficult to extrapolate from this to obtain an estimate of the detection volume of the electrode when many motor units are simultaneously active. To estimate the effective detection radius of the IMES, the EMG signal from simultaneously active motor units was estimated as the radius of active muscle was progressively increased for different orientations of the electrode. It was assumed that the muscle fibers were located sufficiently deep within the limb so that fat and skin tissue did not affect the detected action potentials. However, previous studies have indicated that the presence of highly resistive tissues, such as fat, bone or an insulating medium can cause a distortion of the electric field, when the muscle fiber and detection electrode are sufficiently close to them. As expected, the most selective EMG recordings were observed with the electrode orientated parallel to the muscle fiber direction, Fig. 5. Rotating the electrode 22.5° or 45° with respect to the fiber direction increased the estimated detection radius of the electrode from 4.8 mm, to 6.2 mm, to 7.5 mm, Fig. 5. While the detection radius of the electrode, estimated without consideration of the skin and fat tissue, lies within the radius of several of the forearm muscles, the radii of many of the smaller muscles are comparable to the electrode detection radius, Fig. 6. In these muscles, positioning of the electrode at the center of the muscle and alignment of the electrode along the direction of the muscle fibers will be particularly important to ensure that EMG signals from muscles other than the muscle of interest are minimized. It may, therefore, be preferable to surgically implant the IMES electrodes rather than inject them directly into the muscle. A reduction in the bipolar interelectrode distance has been shown to reduce the pick-up volume of the electrode in surface EMG [5]. A similar interaction between the interelectrode distance and the EMG pick-up volume would be expected here. It is likely that as further generations of implanted sensing devices are developed, smaller interelectrode distances and more focal intramuscular EMG recordings will become possible. Having a broad detection volume may, however, be beneficial from a control perspective as it can provide a more global measure of the activity of the entire muscle.

The models that are presented are simplified representations of the complex muscle activation system. Several factors that influence the selectivity of the electrodes have been discussed, including variations in the electrical properties of the surrounding tissues and motor unit activation patterns. In the examples presented it has also been assumed that all muscle fibers run parallel to one another although many of the fibers within the muscles of the forearm are pennated. Interpretation of the simulation results in a quantitative manner should, therefore, be conducted with caution. Furthermore, as the focus of this present study was the influence of physical factors related to EMG volume conduction, neural control strategies such as co-contraction of forearm muscles have not been addressed. Nevertheless, the simulation results presented provide a qualitative insight into the effects of different factors on the characteristics of EMG signals detected using chronically implanted IMES electrodes and an approximate indication of the volume of muscle which is likely to be detected.

V. Conclusion

The purpose of this study was to test the feasibility of recording independent EMG signals from the muscles of the forearm, for myoelectric prosthetic control, using chronically implanted IMES electrodes. The simulation results suggest that the presence of a thin layer of encapsulation tissue around the IMES should not impede the detection of EMG signals from the surrounding muscle fibers and may in fact cause the amplitude of the EMG signal to increase modestly. The orientation of the bipolar electrode with respect to the fiber direction is an important factor in determining the selectivity of the implanted electrode. Alignment of the electrode along the fiber direction will be particularly important in smaller muscles where the detection volume of the electrode is comparable to the radius of the muscle.

References

[1] R. F. f. Weir, E. C. Grahn, and S. J. Duff, "A new externally-powered, myoelectrically controlled prosthesis for persons with partial hand amputations at the metacarpals," *J. Prosthet. Orthotics.*, vol. 12, pp. 26–31, 2001.

[2] R. Vinet, Y. Lozac'h, N. Beaudry, and G. Drouin, "Design methodology for a multifunctional hand prosthesis," *J. Rehabil. Res. Dev.*, vol. 32, pp. 316–324, 1995.

[3] C. M. Light and P. H. Chappell, "Development of a lightweight and adaptable multiple-axis hand prosthesis," *Med. Eng. Phys.*, vol. 22, pp. 679–684, 2000.

[4] P. J. Kyberd and P. H. Chappell, "The Southampton hand: An intelligent myoelectric prosthesis," *J. Rehabil. Res. Dev.*, vol. 31, pp. 326–334, 1994.

[5] M. M. Lowery, N. S. Stoykov, and T. A. Kuiken, "Independence of myoelectric control signals examined using a surface EMG model," *IEEE Trans. Biomed. Eng.*, vol. 50, no. 6, pp. 789–793, Jun. 2003.

[6] R. F. Weir, P. R. Troyk, G. DeMichele, and T. A. Kuiken, "Implantable myoelectric sensors (IMES) for upper-extremity prosthesis control – Preliminary work," presented at the 25th Annu. Conf. IEEE Engineering in Medicine and Biology Society, Cancun, Mexico, 2003.

[7] J. Kimura, *Electrodiagnosis in Diseases of Nerve and Muscle: Principles and Practice*, 2nd ed. Philadelphia, PA: Davis, 1989.

[8] S. D. Nandedkar, D. B. Sanders, and E. V. Stalberg, "Simulation and analysis of the electromyographic interference pattern in normal muscle. Part II: Activity, upper centile amplitude, and number of small segments," *Muscle Nerve*, vol. 9, pp. 486–490, 1986.

[9] W. M. Grill and J. T. Mortimer, "Electrical properties of implant encapsulation tissue," *Ann. Biomed. Eng.*, vol. 22, pp. 23–33, 1994.

[10] I. Arcos, R. Davis, K. Fey, D. Mishler, D. Sanderson, C. Tanacs, M. J. Vogel, R. Wolf, Y. Zilberman, and J. Schulman, "Second-generation microstimulator," *Artif. Organs*, vol. 26, pp. 228–231, 2002.

[11] P. A. Grandjean and J. T. Mortimer, "Recruitment properties of monopolar and bipolar epimysial electrodes," *Ann. Biomed. Eng.*, vol. 14, pp. 53–66, 1986.

[12] M. M. Lowery, N. S. Stoykov, A. Taflove, and T. A. Kuiken, "A multiple-layer finite-element model of the surface EMG signal," *IEEE Trans. Biomed. Eng.*, vol. 49, no. 5, pp. 446–454, May 2002.

[13] J. R. Brauer and B. S. Brown, *EMAS User's Mannual – Version 4*. Pittsburgh, PA: Ansoft Corp., 1997.

[14] P. Rosenfalck, "Intra- and extracellular potential fields of active nerve and muscle fibres. A physico-mathematical analysis of different models," *Acta Physiologica Scandinavica, Suppl. 321*, pp. 1–168, 1969.

[15] A. A. Amis, D. Dowson, and V. Wright, "Muscle strengths and musculo-skeletal geometry of the upper limb," *Eng. Med.*, vol. 8, pp. 41–48, 1979.

[16] T. Gootzen, D. F. Stegeman, and A. Van Oosterom, "Finite limb dimensions and finite muscle length in a model for the generation of electromyographic signals," *Electroencephalogr. Clin. Neurophysiol.*, vol. 81, pp. 152–162, 1991.
[17] R. Plonsey, "Action potential sources and their volume conductor fields," *Proc. IEEE*, vol. 65, no. 5, pp. 601–611, May 1977.
[18] C. Gabriel, S. Gabriel, and E. Corthout, "The dielectric properties of biological tissues .1. Literature survey," *Phys. Med. Biol.*, vol. 41, pp. 2231–2249, 1996.
[19] N. S. Stoykov, M. M. Lowery, A. Taflove, and T. A. Kuiken, "Frequency- and time-domain FEM models of EMG: Capacitive effects and aspects of dispersion," *IEEE Trans. Biomed. Eng.*, vol. 49, no. 8, pp. 763–772, Aug. 2002.
[20] S. Gabriel, R. W. Lau, and C. Gabriel, "The dielectric properties of biological tissues .2. Measurements in the frequency range 10 Hz to 20 GHz," *Phys. Med. Biol.*, vol. 41, pp. 2251–2269, 1996.
[21] A. V. Sahakian, G. A. Myers, and N. Maglaveras, "Unidirectional block in cardiac fibers: Effects of discontinuities in coupling resistance and spatial changes in resting membrane potential in a computer simulation study," *IEEE Trans. Biomed. Eng.*, vol. 39, no. 5, pp. 510–522, May 1992.
[22] S. D. Nandedkar and E. Stalberg, "Simulation of single muscle fibre action potentials," *Med. Biol. Eng., Comput.*, vol. 21, pp. 158–165, 1983.
[23] S. Andreassen and A. Rosenfalck, "Relationship of intracellular and extracellular action- potentials of skeletal-muscle fibers," *CRC Crit. Rev. Bioeng.*, vol. 6, pp. 267–306, 1981.
[24] M. M. Lowery, C. L. Vaughan, P. J. Nolan, and M. J. O'Malley, "Spectral compression of the electromyographic signal due to decreasing muscle fiber conduction velocity," *IEEE Trans. Rehabil. Eng.*, vol. 8, no. 3, pp. 353–361, Sep. 2000.
[25] F. Buchthal, C. Guld, and F. Rosenfalck, "Multielectrode study of the territory of a motor unit," *Acta Physiol. Scand.*, vol. 39, pp. 83–104, 1957.
[26] F. Buchthal, F. Erminio, and P. Rosenfalck, "Motor unit territory in different human muscles," *Acta Physiol. Scand.*, vol. 45, pp. 72–87, 1959.
[27] M. M. Lowery and M. J. O'Malley, "Analysis and simulation of changes in EMG amplitude during high-level fatiguing contractions," *IEEE Trans. Biomed. Eng.*, vol. 50, no. 9, pp. 1052–1062, Sep. 2003.
[28] H. P. Clamann, "Statistical analysis of motor unit firing patterns in a human skeletal muscle," *Biophys. J.l*, vol. 9, pp. 1233–1251, 1969.
[29] R. L. Lieber, M. D. Jacobson, B. M. Fazeli, R. A. Abrams, and M. J. Botte, "Architecture of selected muscles of the arm and forearm: Anatomy and implications for tendon transfer," *J. Hand Surg. [Am.]*, vol. 17, pp. 787–798, 1992.
[30] H. Gray, *Anatomy of the Human Body*. Philadelphia, PA: Lea & Febiger, 1918.
[31] K. Roeleveld, J. H. Blok, D. F. Stegeman, and A. vanOosterom, "Volume conduction models for surface EMG; Confrontation with measurements," *J. Electromyogr. Kinesiol.*, vol. 7, pp. 221–232, 1997.
[32] J. P. P. van Vugt and J. G. van Dijk, "A convenient method to reduce crosstalk in surface EMG," *Clin.l Neurophysiol.*, vol. 112, pp. 583–592, 2001.

Madeleine M. Lowery (M'00) received the B.E. and Ph.D. degrees from the Department of Electronic and Electrical Engineering, University College Dublin, National University of Ireland, in 1996 and 2000, respectively.

Between 2000 and 2005, she was a Postdoctoral Fellow and then a Research Scientist and Research Assistant Professor at the Rehabilitation Institute of Chicago, Chicago, IL, and the Department of Physical Medicine and Rehabilitation, Northwestern University, Evanston, IL. She is currently a Lecturer in the School of Electrical, Electronic and Mechanical Engineering, University College Dublin and holds an adjunct appointment with the Department of Physical Medicine and Rehabilitation, Northwestern University. Her research interests include mathematical modeling and analysis of bioelectric signals, myoelectric prosthetics, and motor control.

Richard F. *ff.* Weir (M'92) was born in Dublin, Ireland, and received the B.A. degree in mathematics and the B.A.I. degree in microelectronics and electrical engineering from Trinity College, Dublin, in 1983. After working as a control engineer in England, he moved to the USA and received the M.S. and Ph.D. degrees in biomedical engineering from Northwestern University, Evanston, IL.

He is currently a Research Scientist at the Jesse Brown VA Medical Center, Chicago, IL, and holds appointments as a Research Assistant Professor in the Departments of Physical Medicine & Rehabilitation and Biomedical Engineering at Northwestern University. He has research interests in the area of neural control, biomechatronics, and rehabilitation, specifically arm/hand systems, manipulators, robotics, and their associated control. The current focus of this work is the development of a multichannel/multifunction prosthetic hand/arm controller system based on implantable myoelectric sensors (IMES), the development of an externally powered partial hand prostheses the development of a multifunction externally powered prosthetic hand, as well as an exploration of the use of series elastic actuators for use in prosthetic devices.

Todd A. Kuiken (M'99) received the B.S. degree in biomedical engineering from Duke University, Durham, NC, in 1983, the Ph.D. degree in biomedical engineering from Northwestern University, Evanston, IL, in 1989, and the M.D. degree from Northwestern University Medical School in 1990.

He was the Frankel Research Fellow at the Rehabilitation Institute of Chicago, Chicago, IL, in 1992. He completed a residency in physical medicine and rehabilitation at the Rehabilitation Institute of Chicago in 1995. He is currently the Director of the Neural Engineering Center for Artificial Limbs and Director of Amputee Services at the Rehabilitation Institute of Chicago. He is an Associate Professor in the Departments of PM&R and Biomedical Engineering of Northwestern University. He is also the Associate Dean of Academic Affairs at the Rehabilitation Institute of Chicago, Feinberg School of Medicine. His research interests include prosthestic control systems, using nerve-transfers to improve artificial arm function, cutaneous sensory reinnervation, bioelectromagentics modeling, prosthetic design, human gait, and care of the amputee.

Dr. Kuiken is a board certified Physiatrist.